Published in final edited form as:
Science. 2011 April 8; 332(6026): 243–247. doi:10.1126/science.1201475.

Eosinophils sustain adipose alternatively activated macrophages associated with glucose homeostasis

Davina Wu[1], **Ari B. Molofsky**[4], **Hong-Erh Liang**[1], **Roberto R. Ricardo-Gonzalez**[5], **Hani A. Jouihan**[5], **Jennifer K. Bando**[1], **Ajay Chawla**[5], and **Richard M. Locksley**[1,2,3]

[1]Howard Hughes Medical Institute, University of California, San Francisco, 941430795, USA

[2]Department of Medicine, University of California, San Francisco, 941430795, USA

[3]Department of Microbiology & Immunology, University of California, San Francisco, 941430795, USA

[4]Department of Laboratory Medicine, University of California, San Francisco, 941430795, USA

[5]Division of Endocrinology, Metabolism and Gerontology, Department of Medicine, Stanford University School of Medicine, Stanford, California, 94305-5103, USA

Abstract

Eosinophils are associated with helminth immunity and allergy, often in conjunction with alternatively activated macrophages (AAMs). Adipose tissue AAMs are necessary to maintain glucose homeostasis and are induced by the cytokine interleukin-4 (IL-4). Here, we show that eosinophils are the major IL-4-expressing cells in white adipose tissues of mice, and, in their absence, AAMs are greatly attenuated. Eosinophils migrate into adipose by an integrin-dependent process and reconstitute AAMs through an IL-4/IL-13-dependent process. Mice on high-fat diet develop increased body fat, impaired glucose tolerance and insulin resistance in the absence of eosinophils, and helminth-induced adipose eosinophilia enhances glucose tolerance. Our results suggest that eosinophils play an unexpected role in metabolic homeostasis through maintenance of adipose AAMs.

Adipose tissue macrophages have a central role in promoting chronic low-grade inflammation, which contributes to obesity, insulin resistance and type 2 diabetes that characterize the metabolic syndrome (1). Although adipose macrophages from obese animals have a classically activated inflammatory phenotype, adipose macrophages from healthy lean mice have an alternatively activated phenotype (2). Impeding the ability of macrophages to become alternatively activated by disrupting the nuclear hormone receptor peroxisome proliferator-activated receptor-gamma (PPARγ) renders mice susceptible to diet-induced obesity and glucose intolerance (3, 4). Human PPARγ loss-of-function mutations are also associated with insulin resistance and type 2 diabetes (5). PPARγ is induced in macrophages by IL-4 or IL-13, and promotes arginase-1 expression, one of the signature genes in AAMs (6). *In vitro* studies with adipocyte cell lines suggest that adipocytes themselves can be sources of IL-4 and IL-13 (7), but analysis of adipose tissues *in vivo* are needed to ascertain more definitively the source of these cytokines.

Correspondence and requests for materials should be addressed to R. M. L. (locksley@medicine.ucsf.edu).

Author Contributions. D. W., A. B. M., and H.-E. L., were involved with project planning, experimental work, data analysis and manuscript preparation; R. R. R.-G., H.A.J., and J.K.B. performed experimental work; A. C. was involved in project planning; and R. M. L. was involved in project planning, data analysis and manuscript preparation.

Competing interests statement. The authors declare that they have no competing

To begin an unbiased analysis of IL-4-expressing cells in perigonadal white adipose tissue of mice on normal chow diet, we used IL-4 reporter mice (4get mice), which contain a fluorescent GFP reporter downstream of an IRES element following the endogenous *Il4* gene, thus facilitating recognition of IL-4-competent cells *in vivo* as revealed by their fluorescence (8). To ensure minimal manipulation, we first analyzed cells spontaneously migrating out of minced adipose tissue after overnight incubation in media. Although only small numbers of IL-4-expressing (GFP+) CD4 T cells could be recovered, a large population of GFP+ eosinophils, which constitutively express GFP in 4get mice (8,9), were identified (fig. S1A). We next enzymatically digested perigonadal adipose to prepare a stromal/vascular fraction (SVF) and recovered all IL-4-expressing cells for analysis. 90% of the IL-4-competent cells recovered from perigonadal adipose of mice on normal chow diet were eosinophils, with the remainder comprising small numbers of basophils, CD4 T cells and innate helper type 2 cells (Fig. 1A, eosinophil gating in fig. S1B). Similar to the relatively abundant adipose tissue macrophages, adipose tissue eosinophils were CD11b+ F4/80+, but were distinguished both by GFP-expression in 4get mice and by expression of the sialic acid-binding immunoglobulin receptor, Siglec-F (fig. S1, B and C). Analysis of adipose tissues from 4get mice with a *Gata1* promoter mutation that lack eosinophils (ΔdblGATA mice; 10) confirmed that the isolated cells were eosinophils (fig. S1D). Using mice with a knock-in human *CD2* replacement gene at the *il4* start site to mark cells that have recently secreted IL-4 protein (9), we could show that the majority of IL-4-secreting cells in adipose were eosinophils, although the number of IL-4-secreting cells was only a small population of the total GFP+ IL-4-competent cells (fig. S2). Eosinophils up-regulate the inhibitory Siglec-F receptor as they move from blood into tissues (11). As compared to blood eosinophils, adipose tissue eosinophils show increased Siglec-F expression, consistent with tissue residence (fig. S1E). Eosinophils account for 4–5% of the adipose SVF cells, more abundant than total adipose CD4+ T-cells (fig. S1F) or eosinophils in spleen (0.33% ± 0.08%, mean % viable cells ± SEM) or blood (2.4% ± 0.4%, mean ± SEM). Examination of perigonadal adipose by standard histochemistry from wild-type (WT) mice identified eosinophils in normal perigonadal fat (Fig. 1B). Flow cytometric and immunohistochemical examination of adipose tissue from WT, eosinophil-deficient and hypereosinophilic IL-5 transgenic (IL-5tg) mice (12) confirmed that Siglec-F-positive cells with the appearance of eosinophils were present in adipose tissue in numbers that correlated with the eosinophil status of the mice (Fig. 1, C and D). Eosinophils were also identified in perigonadal adipose tissue from wild-type C57BL/6 mice (Fig. 1, E and F). We noted a reciprocal relationship between adipose eosinophils and adiposity, as eosinophils were present but reduced in frequency in C57BL/6 mice fed high fat diet (Fig 1, E and F) or in mice with genetic obesity secondary to leptin deficiency (*ob/ob*, fig S3, A and B), and adipose eosinophil numbers correlated inversely with mouse weight (Fig 1, G and H). Tissue eosinophils with up-regulated Siglec-F were present in perigonadal, subcutaneous, mesenteric and brown adipose tissues; however, the frequency and absolute eosinophil numbers were highest in the metabolically active perigonadal and mesenteric adipose (fig. S3, C and D), tissues with the highest percentage of CD11b+/F4/80+ macrophages (perigonadal 32.4% ± 3.5%; mesenteric 20.7% ± 5.3%; brown 13.8% ± 2.3%; subcutaneous 1.2% ± 0.08%, mean ± SEM).

To determine whether eosinophils migrate into adipose tissue, we transferred splenic eosinophils from hypereosinophilic mice (IL-5tg × 4get) to eosinophil-deficient mice. After three days, eosinophils were recovered from lung, spleen and perigonadal fat. By seven days, however, when eosinophils had declined substantially in lung and spleen, eosinophils remained in stable numbers in adipose tissue (Fig. 2A) and in small intestine (fig. S4). Adoptively transferred eosinophils recovered from adipose tissue up-regulated Siglec-F, consistent with their tissue residence and distinct from the lower amounts of Siglec-F on spleen eosinophils harvested at the same time (fig. S5A). To confirm that eosinophil migration required transit from the blood to adipose tissue, we compared eosinophil

accumulation in tissues of mice treated with antibodies that block VCAM-1- and ICAM-1-mediated migration through α4 and αL integrins expressed on eosinophils (13). As compared with animals receiving isotype control antibodies, anti-integrin treatment blocked accumulation of eosinophils in adipose tissues (Fig. 2B). Conversely, in lung and spleen, where most eosinophils retain low Siglec-F expression and presumably remain within the abundant vasculature of these organs, eosinophils accumulated in animals treated with the anti-integrin antibodies. Anti-integrin antibodies similarly blocked eosinophil migration into adipose tissue after induction of endogenous eosinophilia by IL-25 administration (14; fig. S5, B and C).

Studies of AAMs in adipose have relied on PCR-based detection of signature genes in order to confirm the presence of these cells, but single cell analysis has not been possible. Arginase-1 is a signature gene in mouse AAMs that is induced by IL-4 (6). We isolated cells in perigonadal fat from YARG mice that have a fluorescent reporter introduced into the *arg-1* gene and that can used to identify alternatively activated macrophages *in vivo* (15, fig. S6). In both WT and YARG mice on normal chow diet, total numbers of CD11b+F4/80+ macrophages were similar in adipose (fig. S7), and, in YARG mice, YFP+ macrophages were detected without further manipulation (Fig. 3A, fig. S7A). We used size-gating and Siglec-F expression to confirm that eosinophils do not express YFP fluorescence in YARG mice (fig. S7B). In the absence of IL-4 and IL-13 (16), numbers of total adipose macrophages remained similar (fig. S7C), but numbers of arginase-1-expressing macrophages diminished significantly (Fig. 3, A and B), consistent with a role for these cytokines in sustaining the phenotype of adipose AAMs under homeostatic conditions and in agreement with prior studies using Stat6-deficient mice (3). Unexpectedly, adipose tissues from YARG mice that had been crossed onto the eosinophil-deficient background (YARG × ΔdblGATA) also demonstrated a significant reduction of AAMs in adipose tissue (Fig. 3, A and B) with similar numbers of total macrophages (fig. S7C). To ascertain whether eosinophils are sufficient to sustain AAMs in adipose, we sublethally irradiated eosinophil-deficient YARG mice and reconstituted them with bone marrow cells from hypereosinophilic mice (IL-5tg × 4get). After 4–6 weeks, the perigonadal adipose tissues from reconstituted mice contained GFP+ eosinophils and YFP+ AAMs that were not present in non-reconstituted eosinophil-deficient mice (Fig. 3C). The numbers of eosinophils recovered within the perigonadal adipose tissue of the reconstituted mice correlated with the numbers of arginase-1-expressing macrophages in the same tissue (Fig. 3D). In contrast, animals reconstituted with IL-5tg bone marrow lacking IL-4/13 (IL-5tg × 4/13 DKO) had similar numbers of spleen and adipose tissue eosinophils, as well as similar adipose tissue weights, but did not restore AAMs (Fig. 3E, fig S8, A and B). Thus, eosinophils and hematopoietic cell-derived IL-4/IL-13 are required to sustain adipose AAMs. Supporting these experiments, IL-4 and IL-13 transcripts were found predominantly in the SVF rather than the adipocyte fraction of perigonadal white adipose tissue from WT mice (fig. S8, D and E).

During these experiments, it became apparent that the visceral adipose tissue of hypereosinophilic IL-5tg mice was visually smaller than the same tissues from littermate WT mice when both were fed normal chow diet (Fig. 4A). As compared to WT mice, IL5tg mice had an improved response to a glucose challenge (Fig. 4B). Although differences in adipose tissue weight were not significant in eosinophil-deficient mice maintained on normal chow diet, adiposity was greatly augmented when the mice were put on high-fat diet. Under these conditions, analysis using dual energy X-ray absorptiometry (DEXA) scans demonstrated significant increases in total body fat and percentage fat content in eosinophil-deficient mice as compared to WT littermates maintained on high-fat diet, suggesting a role for eosinophils in protecting against diet-induced obesity (Fig. 4, C and D). The obesity induced in eosinophil-deficient mice on high-fat diet was metabolically relevant because

these mice demonstrated significantly impaired glucose tolerance as compared to WT animals (Fig. 4E). When aged to 20–24 weeks on high-fat diet, eosinophil-deficient mice had normal to mildly elevated levels of fasting insulin (fig. S9A), indicating adequate pancreatic beta-cell insulin production. Eosinophil-deficient mice had elevated fasting blood glucose levels (Fig. 4F), however, and decreased adipose insulin responsiveness, as shown by diminished tissue pAKT levels after insulin challenge (Fig. 4, G and H).

To ask whether physiologic elevations of eosinophils could improve glucose tolerance in the setting of high-fat diet, we infected mice on high-fat diet with a migratory helminth, *Nippostrongylus brasiliensis*. Although the parasite is cleared after 8 days, a sustained metabolic response was seen, characterized by decreased fasting glucose and improved insulin sensitivity and glucose tolerance present early post-infection (Fig. 4, I and J) and sustained up to 35 days post-infection (fig. S9B). Remarkably, decreased perigonadal adipose tissue weight (control 2.4 g ± 0.12; infected 1.8 g ± 0.15, $p<0.01$), and increased perigonadal adipose eosinophils were also maintained up to 45 days post-infection (Fig. 4K), when spleen, liver and bone marrow eosinophils had returned to baseline (fig. S9C). Total adipose macrophages from the infected cohort were also relatively decreased (control 50.6% ± 2.7; infected 35.3% ± 2.0, $p<0.05$), consistent with a decline of classically activated macrophages known to preferentially populate adipose tissue during high-fat feeding (2).

Despite much literature defining a role for AAMs in sustaining insulin sensitivity and glucose homeostasis, the mechanisms responsible for maintaining these cells in healthy adipose tissues are largely unknown. Although differences exist between mouse and human AAMs, including in the expression of arginase-1 as used here, we note the overlapping profiles of IL-4/IL-13-conditioned human monocyte/macrophages that have also allowed recognition of human AAMs (6). Our work suggests eosinophil IL-4 production may contribute to sustaining AAMs; however, additional contributions from eosinophils are likely important, possibly through production of cytokines, chemokines or other mediators. Furthermore, we note that innate helper 2 (ih2) cells, recently implicated as an important source of IL-5 and IL-13, are present in adipose (Fig 1A), as previously noted (17), and future study will be required to address whether cytokines from these cells maintain adipose eosinophil homeostasis. Additional contributions by adaptive immune cells likely add further complexity and fine control (18–20).

Despite their appearance in allergy and states of parasitism, particularly in response to intestinal helminthes, the biologic role of eosinophils remains incompletely defined. Although sparse in blood of persons in developed countries, eosinophils are often elevated in individuals in rural developing countries where intestinal parasitism is prevalent and metabolic syndrome rare (21). We speculate that eosinophils may have evolved to optimize metabolic homeostasis during chronic infections by ubiquitous intestinal parasites (22), and in contrast to the insulin-resistant state induced by acute microbial infections (23). Our findings further support the intertwined relationship between metabolism and immunity (1), and are consistent with the enrichment of inflammatory and immune response genes associated with obesity in humans (24, 25). Modulating adipose eosinophil number and function could provide an exciting and novel therapeutic target in human metabolic disorders.

Supplementary Material

Refer to Web version on PubMed Central for supplementary material.

Acknowledgments

We thank J. Cyster, D. Erle, C. Gerard, J. Lee and A. McKenzie for reagents and mice, N. Flores for animal husbandry, Z. Wang for technical assistance, and M. Anderson and C. Lowell for constructive review of the manuscript. This work was supported by the Howard Hughes Medical Institute and grants from the NIH (AI026918), Juvenile Diabetes Research Foundation Innovative Grant, Larry L. Hillblom Foundation Network Grant and the Sandler Asthma Basic Research Center. Support was provided by the Diabetes Endocrinology Research Center grant DK063720, UCSF MSTP (D.W.), UCSF Dept. of Laboratory Medicine (A.B.M.) and F30 DK083194 from the National Institutes of Health (D.W.). Animal care was in accordance with UCSF LARC committee guidelines.

References and Notes

1. Hotamisligil GS. Inflammation and metabolic disorders. Nature. 2006; 444:860–867. [PubMed: 17167474]
2. Lumeng CN, Bodzin JL, Saltiel AR. Obesity induces a phenotypic switch in adipose tissue macrophage polarization. J Clin Invest. 2007; 117:175–184. [PubMed: 17200717]
3. Odegaard JI, et al. Macrophage-specific PPARγ controls alternative activation and improves insulin resistance. Nature. 2007; 447:1116–1120. [PubMed: 17515919]
4. Bouhlel MA, et al. PPARγ activation primes human monocytes into alternative M2 macrophages with anti-inflammatory properties. Cell Metab. 2007; 6:137–143. [PubMed: 17681149]
5. Jeninga EH, Gurnell M, Kalkhoven E. Functional implications of genetic variation in human PPARgamma. Trends Endocrinol Metab. 2009; 20:380–387. [PubMed: 19748282]
6. Martinez FO, Helming L, Gordon S. Alternative activation of macrophages: an immunologic functional perspective. Annu Rev Immunol. 2009; 27:451–483. [PubMed: 19105661]
7. Kang K, et al. Adipocyte-derived Th2 cytokines and myeloid PPARδ regulate macrophage polarization and insulin sensitivity. Cell Metab. 2008; 7:485–495. [PubMed: 18522830]
8. Mohrs M, Shinkai K, Mohrs K, Locksley RM. Analysis of type 2 immunity in vivo with a bicistronic reporter. Immunity. 2001; 15:303–311. [PubMed: 11520464]
9. Mohrs K, Wakil AE, Killeen N, Locksley RM, Mohrs M. A two-step process for cytokine production revealed by IL-4 dual-reporter mice. Immunity. 2005; 23:419–429. [PubMed: 16226507]
10. Yu C, et al. Targeted deletion of a high-affinity GATA-binding site in the GATA-1 promoter leads to a selective loss of the eosinophil lineage in vivo. J Exp Med. 2002; 195:1387–1395. [PubMed: 12045237]
11. Voehringer D, van Rooijen N, Locksley RM. Eosinophils develop in distinct stages and are recruited to peripheral sites by alternatively activated macrophages. J Leukoc Biol. 2007; 81:1434–1444. [PubMed: 17339609]
12. Lee NA, et al. Expression of IL-5 in thymocytes/T cells leads to the development of massive eosinophilia, extramedullary eosinophilopoiesis, and unique histopathologies. J Immunol. 1997; 158:1332–1344. [PubMed: 9013977]
13. Rothenberg ME, Hogan SP. The eosinophil. Annu Rev Immunol. 2006; 24:147–174. [PubMed: 16551246]
14. Fort MM, et al. Il-25 induces IL-4, IL-5 and IL-13 and Th2-associated pathologies in vivo. Immunity. 2001; 15:985–995. [PubMed: 11754819]
15. Reese TA, et al. Chitin induces accumulation in tissue of innate immune cells associated with allergy. Nature. 2007; 447:92–96. [PubMed: 17450126]
16. McKenzie GJ, Fallon PG, Emson CL, Grencis RK, McKenzie AN. Simultaneous disruption of interleukin (IL)-4 and IL-13 defines individual roles in T helper cell type 2-mediated responses. J Exp Med. 1999; 189:1565–1572. [PubMed: 10330435]
17. Moro, et al. Innate production of T(H)2 cytokines by adipose tissue-associated cKit(+)Sca-1(+) lymphoid cells. Nature. 2010; 463:540–544. [PubMed: 20023630]
18. Nishimura, et al. CD8+ effector T cells contribute to macrophage recruitment and adipose tissue inflammation in obesity. Nat Med. 2009; 15:914–920. [PubMed: 19633658]

19. Winer, et al. Normalization of obesity-associated insulin resistance through immunotherapy. Nat Med. 2009; 15:921–929. [PubMed: 19633657]
20. Feuerer, et al. Lean, but not obese, fat is enriched for a unique population of regulatory T cells that affect metabolic parameters. Nat Med. 2009; 15:930–939. [PubMed: 19633656]
21. Karita E, et al. CLSI-derived hematology and biochemistry reference intervals for healthy adults in eastern and southern Africa. PLoS One. 2009; 4:e4401. [PubMed: 19197365]
22. Hotamisligil GS, Erbay E. Nutrient sensing and inflammation in metabolic diseases. Nat Rev Immunol. 2008; 8:923–934. [PubMed: 19029988]
23. Zu L, et al. Bacterial endotoxin stimulates adipose lipolysis via Toll-like receptor 4 and extracellular signal-regulated kinase pathway. J Biol Chem. 2009; 284:5915–5926. [PubMed: 19122198]
24. Emilsson V, et al. Genetics of gene expression and its effect on disease. Nature. 2008; 452:423–428. [PubMed: 18344981]
25. Chen Y, et al. Variations in DNA elucidate molecular networks that cause disease. Nature. 2008; 452:429–435. [PubMed: 18344982]

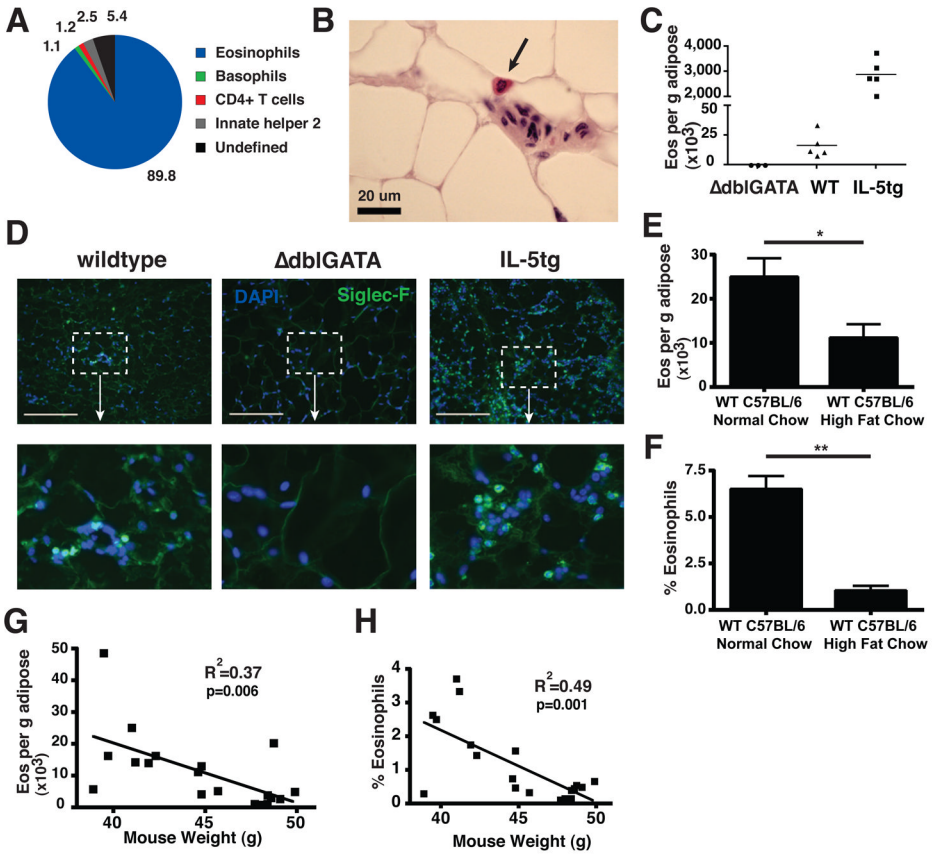

Fig. 1.

IL-4-expressing cells in adipose tissue. (**A**) GFP-positive cells in perigonadal adipose from 4get mice on normal chow. Gating criteria delineated in Supplemental methods and fig. S1B. Data pooled from 3 independent experiments with 2 or more mice per group. (**B**) Hematoxylin and eosin stain of wildtype (WT) paraffin-embedded adipose (scale bar 20 μm), representative of 2 independent experiments. (**C**) Eosinophil numbers as ascertained by flow cytometry in perigonadal adipose from 8 wk-old male mice from ΔdblGATA, WT, and IL-5tg mice on normal chow diet. Data is representative of 3 or more independent experiments. (**D**) Representative immunofluorescent images of Siglec-F+ cells in perigonadal adipose from the strains indicated (scale bar 50 μm). Siglec-F, green; nuclei counterstain with DAPI, blue, representative of 2 experiments. **(E–H)** WT male C57BL/6 mice were fed high-fat diet for 10–14 wk and compared with normal chow WT C57BL/6 controls. Perigonadal adipose eosinophils were quantified by flow cytometry per g adipose tissue **(E)** or percent of total stromal vascular fraction (SVF) cells **(F)**. Correlation is shown between mouse weight on high-fat chow and adipose eosinophil numbers (**G, H**), utilizing Pearson's correlation coefficient. **(E–H)** Results are pooled data from two independent experiments with 20 total mice. *p<0.05, **p<0.01

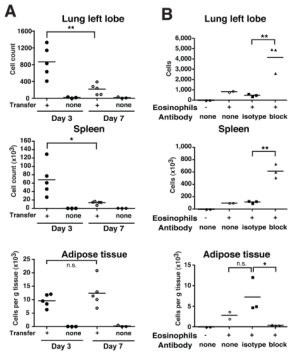

Fig. 2.

Eosinophil migration to adipose tissue is integrin-mediated. (**A**) Eosinophils in the left lobe of the lung, spleen and perigonadal adipose tissue 3 and 7 days after adoptive transfer into eosinophil-deficient ΔdblGATA mice on normal chow. Data shown is pooled from two independent experiments. (**B**) ΔdblGATA mice received antibodies to α4 and αL integrins (100 μg each) or control isotypes (IgG2a and IgG2b) 2 hrs prior to adoptive transfer of eosinophils. Tissues were harvested 16 hrs later. Data shown is representative of two independent experiments. *p<0.05, **p<0.01 as determined using Student's t-test. n.s. = not significant.

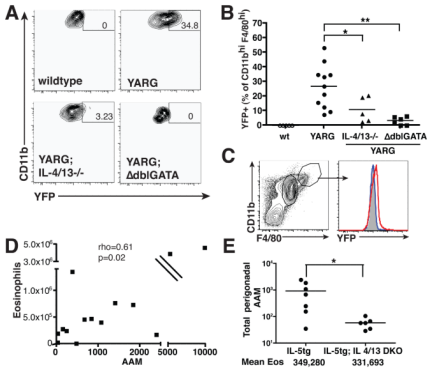

Fig. 3.

Adipose macrophage alternative activation is impaired in the absence of IL-4/IL-13 or eosinophils. (**A**) Flow cytometric analysis of adipose from indicated mice on normal chow diet. Gates show YFP-positive cells as a percent of total CD11b^{high}F4/80^{high} macrophages **(A)** and are quantitated (**B**) Results are pooled data from two or more independent experiments with 2–4 animals per experiment. *p<0.05, **p<0.01 as determined using ANOVA with Bonferonni's post-test correction for multiple comparisons. (**C**) ΔdblGATA × YARG mice were sublethally irradiated and reconstituted with bone marrow cells from 4get × IL-5tg mice. After 4–6 weeks, perigonadal adipose tissues were analyzed for eosinophils (left gate; eosinophils were GFP-positive and side-scatter^{high}, not shown) and macrophages (CD11b^{high} F4/80^{high}, right gate). Macrophages were then analyzed for YFP. Eosinophil-reconstituted mice (red); non-reconstituted mice (blue); WT control (non-reporter) mice (gray). (**D**) Statistical correlation (Spearman's rank correlation) between the total numbers of eosinophils reconstituting perigonadal adipose tissues in eosinophil-deficient mice and the total numbers of AAM expressing the marker arginase-1 allele. Results are pooled data from 5 independent experiments with 2–4 animals per experiment. (**E**) Mice reconstituted with IL-5tg bone marrow lacking IL-4 and IL-13 (IL-5tg × 4/13 DKO) display significantly fewer total YARG+ AAM (**E**) or total YARG+AAM per 1,000 tissue eosinophils (IL-5tg 2.5 ± 1.1; IL-5tg × 4/13 DKO $2.4\times10^{-4} \pm 6.2\times10^{-5}$). Results are pooled data from two or more independent experiments with 2–5 animals per experiment. *p<0.05, **p<0.01 as determined using Student's t-test.

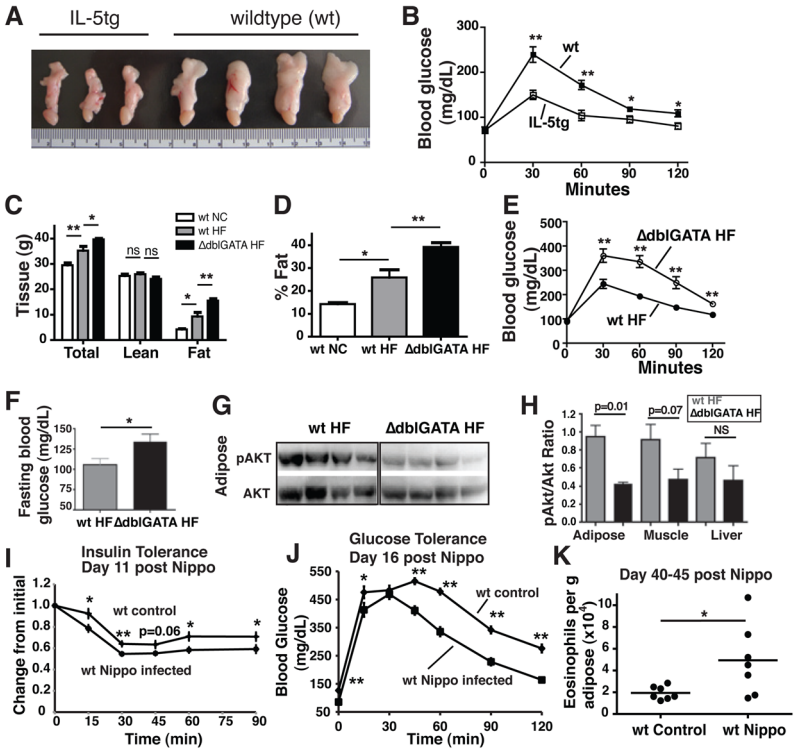

Fig. 4.

Metabolic analysis of eosinophil-deficient and hypereosinophilic mice. (**A**) Perigonadal fat tissues (testis attached) from IL-5 transgenic (IL-5tg) and wildtype (WT) littermate controls. (**B**) Fasting male 8 wk-old WT or IL-5tg littermates maintained on normal chow (NC) diet were challenged with intraperitoneal glucose and blood was sampled for glucose at times indicated. Data compiled from two independent experiments with 6–7 mice in each group. (**C,D**) DEXA analysis of total, lean and fat tissue composition **(C)** or percentage adiposity **(D)** in ΔdblGATA and wildtype (WT) mice on normal chow (NC) or high-fat (HF) diet for 15 wk. Data compiled from two experiments with 5–8 mice in each group. (**E**) Intraperitoneal glucose tolerance test in male ΔdblGATA and WT mice on HF diet for 15 wk. Data compiled from 3 independent experiments with 5–8 mice in each group. (**F**) Fasting blood glucose in male WT and ΔdblGATA mice maintained on HF diet for 20–22 wk. Data compiled from 2 independent experiments with 5 mice in each group. (**G, H**) Insulin signaling, as measured by the ratio of serine phosphorylated AKT to total AKT in adipose, muscle and liver of mice aged 24 wk on HF diet (n = 4–6 mice per genotype, 4 representative mouse adipose samples shown). (**I, J**) Twelve-wk old wild-type C57BL/6 mice on HF diet for 6 wk were infected with *N. brasiliensis* (Nippo) or unchallenged (Control) and monitored for insulin tolerance (**I**) and glucose tolerance (**J**) at the indicated times. Insulin tolerance results are normalized to baseline fasting glucose, which was statistically different between cohorts (WT control 207 mg/dL ± 6; Nippo 179 mg/dL ± 7; $p < 0.05$). (**K**) Adipose tissue collected at days 40–45 post *N. brasiliensis* infection or from uninfected control mice and analyzed by flow cytometry for eosinophils per g adipose (**K**) or percent eosinophils (WT Control 2.9% ± 0.41; Nippo 10.1% ± 0.36, $p<0.01$). Data (**I, J, K**) are representative of two independent experiments with 20–30 total mice per cohort. *$p<0.05$, **$p<0.01$ as determined using Student's t-test (**B, E, F, H–K**) or ANOVA with Bonferroni's post-test correction for multiple comparisons (**C–D**); error bars = SEM; n.s. = not significant.